Miniature Mechanically Pumped Loop for Standardized Small-Satellite Thermal Control: In-Orbit Demonstration Model Development and Qualification

Thomas Ganzeboom MSc.
R&D Engineer
Royal Netherlands Aerospace Centre
Marknesse, The Netherlands
thomas.ganzeboom@nlr.nl

Charlton Castro MSc.
R&D Engineer
Royal Netherlands Aerospace Centre
Marknesse, The Netherlands
charlton.castro@nlr.nl

Ir. Johannes van Es
Principal investigator
Royal Netherlands Aerospace Centre
Marknesse, The Netherlands
johannes.van.es@.nlr.nl

Sybren de Jong MSc.
Principal R&D Engineer
Royal Netherlands Aerospace Centre
Amsterdam, The Netherlands
sybren.de.jong@nlr.nl

***Abstract*—With the rapid growth of the space economy, the demand for increasingly high-performance satellites has risen significantly. The need for increased performance is typically accompanied by higher power consumption, leading to elevated heat generation and challenging thermal environments onboard spacecraft, particularly for small satellites with limited thermal margins. As a result, new thermal control concepts are required to accommodate higher heat loads and heat fluxes while remaining compatible with small-satellite constraints.**

This work presents the next development stage of a novel thermal control concept: the mini Mechanically Pumped Loop (miniMPL). The miniMPL is intended as a standardized thermal control solution for small satellites and is designed to be lightweight, power-efficient, and inherently redundant, while maintaining orbit-independent performance.

We report on the design, manufacturing, and qualification testing of the first Flight Model of the miniMPL, developed for an in-orbit technology demonstration scheduled for launch later this year. The Flight Model has successfully completed a comprehensive environmental test campaign, including vibration, electromagnetic compatibility, and thermal vacuum testing, demonstrating its readiness for spaceflight.

Keywords—*Small satellite thermal control, mechanically pumped loop, CubeSat, two-phase accumulator, piezoelectric pump, spacecraft thermal management*

I. INTRODUCTION

The rapid growth of the small satellite market has led to increased onboard power densities that challenge conventional passive thermal control approaches [1]. Active thermal control systems are therefore required to handle the higher heat loads while remaining compatible with CubeSat- and small satellite class constraints. The miniMPL concept addresses this need through a compact, redundant mechanically pumped loop architecture specifically adapted for CubeSat- and small satellite-class constraints.

Following the Engineering Model (EM) development [2], the next step is flight qualification and in-orbit demonstration. This Flight Model validates environmental compatibility, manufacturability, and system-level performance under representative mission conditions.

In contrast to conventional pumped-loop systems used on large spacecraft, the miniMPL concept is specifically tailored to the mass, volume, and power constraints of small satellite platforms. To the authors' knowledge, this represents one of the first reported integrated mechanically pumped loop demonstrations fully contained within a 1U CubeSat payload volume. The presented Flight Model therefore represents an important step toward making active thermal control available to a class of spacecraft that has historically relied almost exclusively on passive methods.

This paper describes the miniMPL technology, the key improvements made from the Engineering Model to Flight Model, and the results of the flight qualification test campaign.

II. FLIGHT MODEL REQUIREMENTS

A. *Mission Overview*

The in-orbit demonstration will be performed on the Horizon Europe CASSINI-IOD-IOV IHE-1 mission, a 6U CubeSat mission to Low Earth Orbit (LEO). The miniMPL system has been given a 1U slot within the CubeSat. Within the mission architecture, the miniMPL system will be operated as an independent thermal control experiment. A controlled dummy heat load will be actively cooled by the system, with the heat rejected through a dedicated radiator.

During the mission, several modes of operation will be tested. The thermal response of the system, as well as its stability and performance will be monitored through onboard telemetry and logged for post-flight analysis. The resulting data will be used to validate system behaviour in a representative space environment, improve performance predictability, and further de-risk the miniMPL for future commercial applications.

B. *Flight Model Performance Requirements*

The performance requirements for the Flight Model were primarily driven by platform constraints, while maintaining a representative full-scale miniMPL thermal control system configuration.

1) Power consumption: The orbit-average power consumption is limited to 5 W, as dictated by platform constraints. This maximum includes the total electrical power required for pump operation, drive electronics, and heaters on both the accumulator and the dummy heat source. The limitation necessitates operation at reduced performance levels compared to the full system capability. The peak power consumption is limited to approximately 7 W.

2) Heat transport capability: The miniMPL In-Orbit Demonstration Flight Model is capable of transporting up to 40 W per pump assembly. However, due to the limited available electrical power on the demonstration platform, the maximum heat transport to be demonstrated is limited to approximately 5 W. To keep the model representative of a commercial thermal control system, a full-scale system configuration was selected for flight despite the resulting under-utilisation of its capacity.

3) Maximum volume: The total allocated volume for the Flight Model is limited to 1U, which is based on the available space within the CubeSat platform. This volume includes not only the miniMPL itself but also the drive electronics, a dedicated dummy heat load and radiator. These volume limitations enforce a compact and integrated design.

4) Maximum mass: The total system mass is limited to 1 kg, as defined by platform constraints. In previous works *[2]* it was demonstrated that this mass budget is sufficient to accommodate all required components, including the pump, accumulator, tubing, heat exchangers, and supporting structure.

C. Environmental and qualification requirements

The mission to LEO imposes a range of mechanical, thermal, and electromagnetic environmental conditions. These conditions were incorporated into the design and qualification stages of the miniMPL Flight Model development. The system was qualified in accordance with applicable ECSS standards.

The miniMPL system was tested at Proto Flight Model (PFM) level as a separate subsystem. This approach combined qualification and acceptance testing of the miniMPL while minimizing the required number of test campaigns and ensuring that the hardware is representative of the final flight configuration. After this, the entire CubeSat will undergo acceptance-level environmental testing. These system-level tests fall beyond the scope of this paper, as they have not yet been completed at the time of writing.

1) Launch loads: During launch, the miniMPL system will be subjected to mechanical loads induced by the launch vehicle. The qualification levels are based on the expected launch environment generated by the Rocket Factory Augsburg (RFA) RFA-one launch vehicle. The vibration levels are described below and are applied in all three principal axes of the miniMPL system.

a) Sine vibration: Sine vibration testing was performed to simulate low-frequency launch loads and structural resonances, see Table I.

TABLE I. SINE VIBRATION LEVELS

Frequency range:	2-100 Hz
Acceleration Level:	2-50 Hz @1.25 g 50-100 Hz @1.125 g
Sweep rate:	4.0 oct/min

b) Quasi-static loading: Quasi-static loads represent sustained accelerations experienced during launch, such as those induced by rocket engine thrust. In the test campaign this load was applied as a 20 Hz sine dwell to emulate the quasi-static load, see Table II.

TABLE II. QUASI-STATIC LOAD LEVELS

Acceleration	±7.25 g
Duration	30 seconds
Frequency	20 Hz

c) Random vibration: Random vibration testing simulates the broadband dynamic environment experienced during launch, primarily caused by engine noise and aerodynamic effects, see Table III.

TABLE III. RANDOM VIBRATION LEVELS

Frequency	**Spectral density [g^2/Hz]**
20	0.010
100	0.024
600	0.022
900	0.014
2000	0.014
GRMS [g]	**5.78**

2) Thermal vacuum environment: Once in LEO, the miniMPL system will experience a high vacuum environment as well as cyclic temperature conditions. Thermal vacuum testing was performed to qualify the miniMPL system for this specific environment. The objectives of the thermal vacuum testing were:

- Verification of leak-tight design of the system under vacuum
- Demonstration and validation of system operation under cyclic temperature conditions

The test campaign includes both operational and survival temperature conditions. During operational testing, the system was powered and required to demonstrate nominal performance over the full temperature range. During survival testing, the system was not powered and exposed to more extreme temperatures to verify structural and functional integrity.

The temperature range used for operational and survival testing is shown in Table IV. The maximum temperature during survival testing required by specification is 65°C, however it was decided to combine this part of the test with a bake-out at 80°C for 16 hours.

TABLE IV. THERMAL VACUUM TEST ENVIRONMENT

Mode	**T_{min}**	**T_{max}**	**# Cycles**	**Rate**	**t_{dwell}**
Operational	-20 °C	+50 °C	4	2 °C/min	2 hours
Survival	-40 °C	+80 °C	1	2 °C/min	2 hours[a]

[a] The hot dwell for the survival test was 16 hours, to act as a bake-out.

3) Electromagnetic compatibility (EMC): The miniMPL design includes active drive electronics to operate the piezoelectric pump. The electronics must be compliant with

EMC requirements so as not to interfere with other systems on the same platform. The EMC requirements for this specific in-orbit demonstration mission are derived from ECSS-E-ST-20-07C with a focus on emission control. As such, the following EMC aspects require verification by testing:

- Conducted emissions
- Radiated emissions

The miniMPL pump drive electronics are designed to be robust with substantial design margins based on heritage design practices, consistent with ECSS standards. For this reason, the system contains only discrete components and legacy logic integrated circuits for its critical function and external interfaces. Susceptibility verification was therefore limited to analysis to minimize the total number of tests.

III. FLIGHT MODEL DESIGN

A. *Flight Model Architecture*

The Flight Model (FM) of the mini Mechanically Pumped Loop (miniMPL) was designed as a compact and integrated thermal control system. Its core components are the pump, drive electronics, and an accumulator. For the purpose of the in-orbit demonstration, a representative heat source, fluid transport tubing and dedicated radiator are also part of the design. In operational applications, the heat source would be payload components that require thermal control. Together these components form a closed loop system enabling active heat transport from the heat source to the radiator.

The overall design philosophy of the miniMPL Flight Model was to maximize thermal performance per unit mass and volume while maintaining simplicity and fault tolerance. Wherever possible, passive robustness was preferred over complex control strategies, resulting in a system architecture that is compact, scalable, and compatible with a wide range of small satellite missions.

The accumulator operates on a two-phase equilibrium in which controlled fluid evaporation sets system pressure through temperature regulation, eliminating the need for a dedicated pressure sensor.

The loop design was specifically developed for this demonstration mission and is based on the Engineering Model design, albeit with some improvements. The architecture can be adjusted according to future mission parameters. Figure 1 shows a schematic depiction of the loop and components involved.

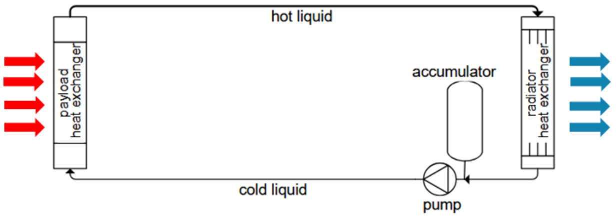

Figure 1. Simplified schematic of the single-phase miniMPL architecture for the in-orbit demonstration mission. Image adapted from [3].

B. *Working fluid selection*

The working fluid of choice is Galden HT55, as it already has heritage with previous iterations of the miniMPL and has demonstrated compatibility with all components. In addition, the boiling point at ambient pressure of 55 °C ensures a relatively low to moderate system pressure at the expected operating temperatures. Galden HT55 was also chosen for its radiation stability and low freezing point of -110 °C, making it well suited for space applications.

C. *Pump assembly design*

The pump assembly forms the core of the miniMPL system and is responsible for generating the required liquid flow through the loop. The pump design is based on the Multi-Parallel Micro-Pump (MPMP) concept which uses oscillating piezoelectric elements to generate flow. The system uses check valves and is driven at 100 Hz to generate continuous circulation.

1) Pump design changes: The EM pump successfully demonstrated the feasibility and performance of the pump concept *[2]*. The FM pump builds upon the lessons learned from the EM pump and incorporates several design improvements to increase reliability and ease of assembly and integration.

a) Piezo wiring: One of the primary improvements concerns the electrical connection between the piezo elements and the external connector. In the Engineering Model individual wires were directly connected to the connector, resulting in a complex and time-consuming assembly procedure. In addition, the relatively long wire lengths increased the risk of assembly errors and mechanical damage during integration. In the Flight Model design, this approach has been replaced by introducing a printed circuit board (PCB). The piezo elements are now connected to the PCB using short wire connections to solder pads. The PCB has traces to electrically connect the piezo elements to the external connector. The PCB designed for this purpose can be seen in Figure 2. This modification significantly reduces wiring complexity and the effort required to integrate the pump.

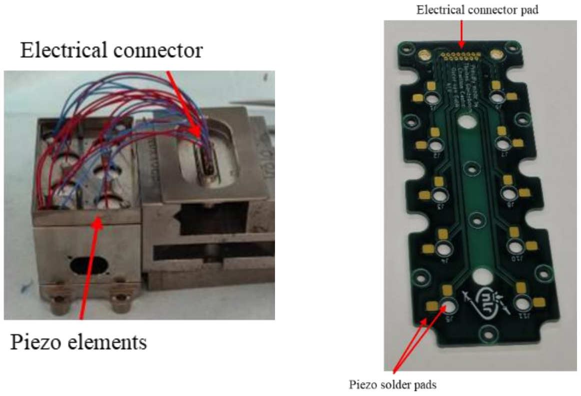

Figure 2. Left: EM integration with long piezo wires. Right: FM PCB replacing long internal wiring.

b) Pump housing material: A second major design change is the material from which the pump is manufactured. The EM was constructed out of titanium grade 5, offering significant weight advantages. However, during integration it was found that welding the pump assembly to the titanium tubing introduced challenges in achieving consistent weld quality and sufficient joint strength.

For the Flight Model, stainless steel has been selected as the structural material for the pump. Although this results in a mass increase, the improvement in weld quality, reliability and strength were considered preferable. This change contributes directly to a more reliable and reproducible assembly process.

c) Pump internal layout: The final improvement made concerns the internal layout of the pump. The Engineering Model pump was designed with minimizing internal pump volume in mind. As a result, the internal layout was very efficient; however it was challenging to place this pump geometry in a CubeSat form factor. The pump layout in the Flight Model has been simplified by placing all piezo elements in a single plane and the inlet/outlet tubes have been moved. This results in a slightly larger pump compared to the EM, however it now fits more efficiently in a CubeSat form factor resulting in more efficient use of available space.

2) Flight Model Pump design: The FM pump keeps the piezo operated core, with 2 piezo elements placed in series forming a pump unit. Five pump units are then placed in parallel to form the overall pump. This is schematically shown in Figure 3. In total, ten piezoelectric elements are used in each pump, providing inherent redundancy and mitigating single-point failure modes. For example, failure of a single piezo would reduce the performance of the pump by at most 10%.

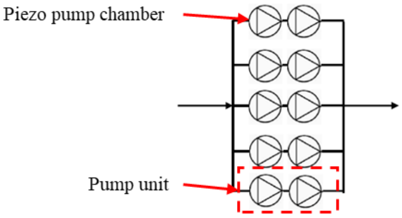

Figure 3. Schematic design of MPMP concept showing 2 piezo operated chambers in series, and 5 pump units in parallel.

The Flight Model pump housing is manufactured from 316L stainless steel using additive manufacturing, enabling integrated internal flow channels while maintaining weldability and mechanical robustness. Critical interfaces were post-machined to final tolerances and improved surface finish, see Figure 4.

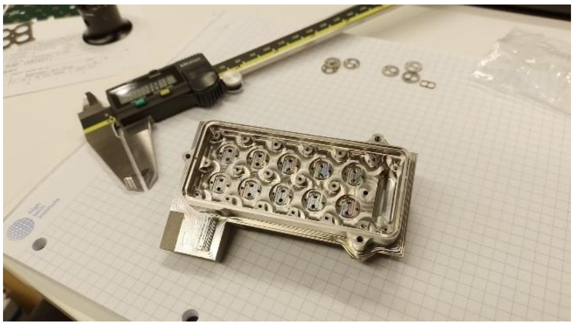

Figure 4. miniMPL Flight Model pump block during machining into final geometry.

The pump body is designed to accommodate ten piezo chambers, internal fluid channels, electrical routing, and the external connector interface. The external connector, also manufactured from 316L stainless steel, is laser welded to the pump housing. A corresponding lid is welded to the main body to achieve a hermetically sealed assembly. The geometry of both the lid and the connector interface has been specifically designed to ensure that mechanical loads are not transferred through the welds. Instead, loads are carried through dedicated mechanical interfaces, such as bolted connections to the baseplate and threaded connector interfaces, thereby reducing the risk of weld failure during launch and operation.

The fluidic interface consists of ¼” outer diameter inlet and outlet tubes, which are directly integrated into the printed pump body and subsequently machined to final dimensions. The internal flow channels are designed with a diamond-shaped cross-section, a geometry selected for reliable additive manufacturing, as fully circular or square cross-sections are more difficult to produce without support structures or post-processing complications.

Each pump chamber uses a layered internal stack consisting of check valves, sealing elements, preload components, and a piezoelectric actuator, as shown in Figure 5. The configuration was optimized for repeatable assembly, leak-tightness, and controlled actuator preload.

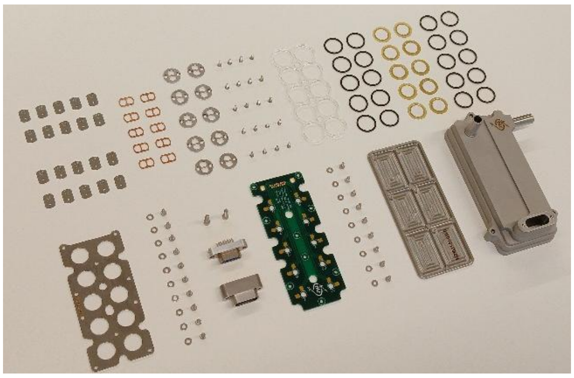

Figure 5. miniMPL Flight Model pump exploded view, showcasing all the individual components that are used inside. Order of assembly is top left to bottom right.

Finally, the printed circuit board (PCB) is integrated into the pump assembly. Openings in the PCB allow the piezo wiring to pass through, enabling short electrical connections that are soldered directly onto the board as shown in Figure 6. This arrangement minimizes wiring complexity and improves assembly repeatability, while maintaining a compact and robust internal layout.

Figure 6. miniMPL Flight Model pump fully assembled except for the lid. Clearly visible are the wires connecting the piezo elements to the PCB.

Performance testing was performed on the integrated pump as a standalone component. This was done in a test bench where the pump was placed in series with a flow meter and variable flow restriction. The flow generated by the pump was measured for various setpoints of the flow restriction. At the same time the pressure head of the pump was recorded. This resulted in a pump curve which shows the generated mass flow versus pressure head of the pump, as shown in Figure 7. It can be seen that the pump has a maximum pressure head of

300 mbar at zero flow and a maximum measured flow of 1.2 g/s at the lowest pressure head.

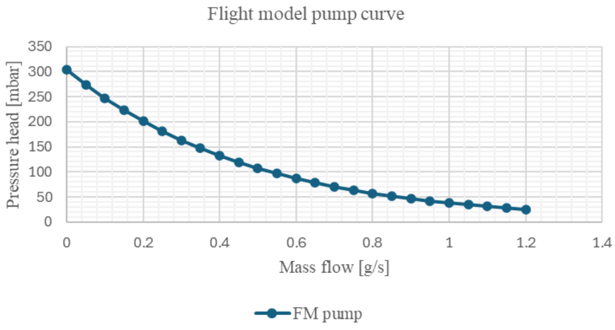

Figure 7. miniMPL Flight Model pump standalone pump curve.

The measured pump performance confirms that the piezoelectric pump of the Flight Model is capable of generating meaningful loop flow and pressure head within a compact package.

In the integrated loop, the operating point is determined by the intersection of the pump curve with the system pressure losses. For the Flight Model configuration, it is expected that the total system pressure drop is about 50 mbar. This results in an expected operating flow rate in the range of 0.8 to 1 g/s. For Galden HT55 at a mass flow of 1 g/s, the fluid temperature rise is approximately 5 °C for a 5 W heat load.

Under the expected environmental conditions, the fluid temperature will be at most 80 °C corresponding to an operating pressure of 2.8 bara based on the Galden HT55 vapour pressure characteristics. The pump housing has been designed to withstand at least 10 bara of system pressure. The minimum and maximum operating temperatures of the pump are determined by the piezo elements used which have a lower temperature limit of -30 °C and an upper limit of 90 °C.

D. *Thermal control components*

In addition to the pump assembly, the miniMPL Flight Model incorporates several thermal control components that together enable controlled heat transport and rejection. These include the accumulator, dummy heat source, radiator, and fluid tubing. Each component has been designed to ensure compatibility with the flight environment while maintaining overall system performance, robustness, and ease of integration.

1) Accumulator: The accumulator is responsible for regulating the system pressure and accommodating expansion and contraction of the working fluid. Maintaining a controlled loop pressure is essential to prevent boiling of the working fluid at the heat source and to avoid cavitation at the pump inlet.

The operating principle of the accumulator is based on a two-phase equilibrium. A portion of the working fluid is allowed to evaporate within the accumulator, thereby generating the required system pressure. Since boiling point and pressure are directly linked, the accumulator can be controlled through its temperature, eliminating the need for a pressure sensor. A heater is attached to the accumulator to provide the thermal input necessary for controlled evaporation. To prevent vapor from entering the liquid loop, a porous wick is placed at the entrance.

The accumulator is mechanically supported by three titanium flexures that provide structural stiffness while minimizing conductive heat transfer, as shown in Figure 8.

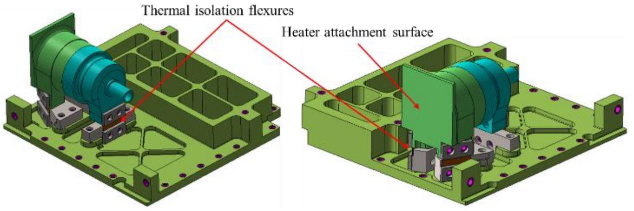

Figure 8. 3D CAD graphic showing miniMPL Flight Model accumulator mounted on the miniMPL Flight Model baseplate. Other components are excluded in this view.

The design temperature of the accumulator is set to at least 20 °C above the highest loop temperature, based on vapor-pressure margin analysis. This ensures that the saturation pressure in the accumulator remains well above the local vapor pressure throughout the loop under all operating conditions. Thermal modelling showed that with these thermal isolation methods, this results in a required heater power of 900 mW.

The heater itself is an electrical resistive element and is placed on the back side of the accumulator, where a flat surface is created for attachment. Thermal paste is used to ensure effective heat transfer between the heater and the accumulator body. Epoxy is used to guarantee mechanical attachment of the heater to the accumulator.

2) Dummy heat source: The dummy heat source represents a controlled thermal input to the miniMPL system and serves as a stand-in for a representative payload during the in-orbit demonstration. Its primary function is to introduce a known and adjustable heat load into the loop, allowing the thermal performance and response of the system to be evaluated under flight conditions.

The heat source is comprised of two electrical resistive elements that are together capable of generating a maximum of 5 W of heat. They are attached to a heat exchanger with thermal paste and epoxy is used to ensure a strong mechanical interface. The heat exchanger that transfers the heat from the heaters to the fluid was designed to be low-complexity as it is only a stand-in for an actual payload. Its design is shown in Figure 9.

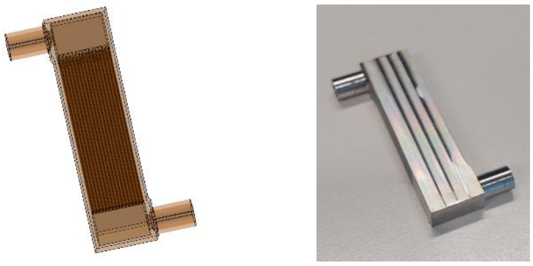

Figure 9. miniMPL Flight Model dummy heat source internal design (left), production part (right).

The internals consist of a fluid manifold that divides the working fluid through several parallel channels. The block is manufactured by SLM metal printing and then machined to its final shape.

3) Radiator: The radiator rejects transported heat to space and closes the thermal loop. Due to constrained available CubeSat surface area, the demonstration radiator is mounted on one spacecraft side and sized for 5 W rejection at an operating temperature of 55 °C, sufficient for the in-orbit demonstration.

Rather than attaching a separate heat exchanger to the radiator surface, an integrated radiator design has been implemented. The radiator panel incorporates internal fluid channels and heat transfer promoting features, allowing direct heat exchange between the working fluid and the radiating surface. This approach reduces thermal interfaces and improves overall thermal efficiency. The internal geometry is based on the offset strip fin design as described in [4] and can be seen in Figure 10.

The radiator is made from 316L stainless steel and the radiative surface is coated with Nextel Velvet Coating 811-21, which is optimized for high emissivity in infrared wavelengths and is commonly used in space applications. The panel is positioned such that it has an unobstructed view to deep space, i.e. minimizing exposure to direct solar and Earth infrared flux.

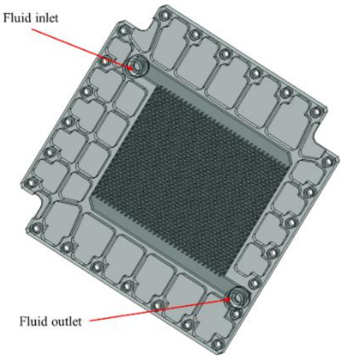

Figure 10. Integrated radiator with internal offset-strip-fin channels enabling direct fluid-to-panel heat transfer. Mass saving recesses are also visible surrounding the heat exchanging area.

Although sized for the constraints of the present demonstration mission, the radiator design is inherently scalable. Larger panel areas or deployment concepts can be implemented in future missions while retaining the same core loop architecture.

4) Fluid tubing: The fluid tubing connects all components of the miniMPL Flight Model into a closed-loop system, enabling the transport of heat from the dummy heat source to the radiator. The tubing is manufactured from 316L stainless steel, consistent with the material selection of the pump, radiator, and other fluidic components. This uniform material choice simplifies manufacturing and ensures compatibility during welding, resulting in robust and reliable connections throughout the system.

The tubing has an outer diameter of 1/4" with wall thickness of 0.9 mm, which is selected as a trade-off between minimizing pressure drop, maintaining compatibility with the compact CubeSat form factor, and weldability of the tube. The total tube length is approximately 20 cm. All connections are realized through orbitally welded joints to ensure leak-tightness and suitability for vacuum operation.

The routing of the tubing has been designed to minimize sharp bends and mechanical stress concentrations, improving structural integrity under launch loads. Additionally, the layout is optimized to limit pressure losses within the loop, ensuring that the pump operates within its optimal performance range.

E. Drive electronics and temperature acquisition

The drive electronics are responsible for actuating the piezo elements within the pump. Each piezo element is driven by an electrical signal that induces cyclic deformation, resulting in a volumetric displacement of the working fluid. The detailed electronics design is described in [5].

The drive electronics generate a high-voltage oscillating signal to actuate the piezo elements. The operating frequency is set to 100 Hz and was selected to achieve optimal pump performance, based on characterization performed during the Engineering Model phase. In the Flight Model, the control philosophy is intentionally kept simple: the pump operates at a fixed frequency and voltage during nominal operation, without active flow control. This approach reduces system complexity and increases robustness for the in-orbit demonstration.

The drive electronics are powered by the spacecraft platform. The primary control functionality consists of switching the pump modules on and off through a logic high/low signal. Telemetry is returned to the OBC to monitor system health, including parameters such as voltage, current, and temperatures.

The electronics design prioritizes reliability and fault isolation. Each piezo channel is electrically isolated to prevent failure propagation, ensuring that a malfunction in a single element does not compromise overall system operation. The architecture is consistent with the design philosophy of the miniMPL system, emphasizing modularity, redundancy, and robustness. The physical layout is configured such that it is compatible with most CubeSat platform mounting types as can be seen in Figure 11.

In addition to the drive electronics, temperature sensors are distributed throughout the miniMPL system to provide insight into both system health and thermal performance during operation. These sensors enable monitoring of temperature within the loop, allowing assessment of heat transport, temperature gradients, and overall system behaviour in-orbit.

Thermistors are placed at the following locations:

- Dummy heat source fluid inlet
- Dummy heat source fluid outlet
- Pump baseplate
- Radiator panel
- Accumulator heater

The collected temperature data is used to evaluate system performance, including heat transfer efficiency and thermal stability under varying operating conditions. Performance characteristics obtained include delta-T across the dummy heat source, radiator effectiveness, and general loop temperature stability.

Figure 11. miniMPL Engineering Model PCB [5]. For the Flight Model the adjustable resistors (blue) and silkscreen are removed and a layer of conformal coating is applied.

a) Power budget: The electrical components each require some power to operate. In Table V the power budget for the full system is given. The power budget shows that the dummy heat can consume up to 5 W of electrical power. This is the value for 100% duty cycle, and is reduced to a nominal value of 3.1 W to comply with the available power on the satellite.

TABLE V. miniMPL SYSTEM IN-ORBIT DEMONSTRATION POWER BUDGET

Component	**Power usage**
Pump drive electronics	1 W
Accumulator heater	0.9 W
Dummy heat source nominal	3.1 W (5 W peak)
Total	**5 W (6.9 W peak)**

F. Control software architecture

The miniMPL does not contain a dedicated onboard controller; control software runs on the spacecraft OBC using three operational states: OFF, IDLE, and EXPERIMENT. Configuration parameters are managed through a centralized Configuration Register Table (CRT), while background services perform telemetry acquisition, health monitoring, and hardware actuation. In EXPERIMENT mode, the software autonomously controls the pump, heater duty cycles, and safety logic. Fault detection is based on telemetry threshold monitoring, with predefined transitions to IDLE or OFF in case of anomalies.

IV. FLIGHT MODEL INTEGRATION

Beyond component-level functionality, successful implementation of mechanically pumped thermal control systems on small satellites depends strongly on manufacturability, ease of integration, and compatibility with standard spacecraft interfaces. To demonstrate this, the Flight Model was developed as an integrated payload rather than as a laboratory breadboard.

For the in-orbit demonstration the miniMPL Flight Model will be integrated into a 6U CubeSat platform as a self-contained payload within a 1U allocated volume. The system is designed to interface with the spacecraft on mechanical, thermal, and electrical levels, while maintaining a high degree of independence to simplify integration and reduce risk.

A. miniMPL mechanical integration

The miniMPL system consists, at its core, of the pump and accumulator, which are integrated into a single equipment block mounted on a common support plate. This support plate provides structural rigidity and ensures a well-defined relative positioning of the components.

The pump inlet is connected to the accumulator through a tee-junction, forming a compact and integrated fluidic assembly. This configuration results in a simplified interface to the remainder of the loop, with a single inlet and outlet tube connecting the equipment block to the dummy heat source and radiator. The overall layout minimizes tubing length and reduces the number of welds required, thereby lowering the risk of leakage and simplifying assembly. A 3D CAD representation of this configuration is shown in Figure 12.

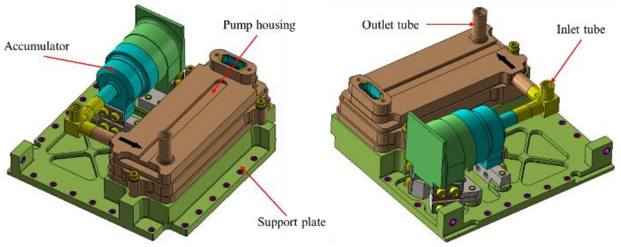

Figure 12. miniMPL Flight Model equipment block showing the accumulator and pump on the integrated support plate.

The support plate is mounted to the CubeSat primary structure through multiple bolted interfaces. The pump housing is mounted in such a way that structural loads are not transferred through welds or fluidic connections, but instead through dedicated mechanical interfaces.

During assembly, dedicated fixtures are used to control alignment of the fluidic interfaces prior to welding. This minimizes residual stresses in the tubing and reduces the likelihood of misalignment-induced loads. The routing of the tubing is designed to avoid unsupported bends in the tube and instead uses pre-manufactured corner pieces, which are then welded to straight sections. Using sharp corner pieces instead of bent tube slightly increases hydraulic resistance of the loop, but improves reliability and reproducibility.

From a thermal perspective, the support plate provides a defined interface to the spacecraft, while the accumulator is intentionally thermally isolated through its titanium blade mounting. This ensures that the thermal behaviour of the accumulator is dominated by its internal heater rather than conductive coupling to the spacecraft structure.

The drive electronics PCB is mounted to the side of the base support plate. In typical miniMPL applications the PCB would be mounted in the same plane as the support plate to minimize used volume. However, due to platform constraints and harness routing through the CubeSat platform, a different location was chosen.

The radiator plate is mounted on the opposite side of the support plate, as this face provides the most favourable view factor for heat rejection. The dummy heat source is placed between the pump outlet and radiator inlet, minimizing interconnecting tube length.

Between the outlet of the radiator and the inlet of the pump a fill line is installed, which allows for filling of the loop. This is further explained in Section IV.B.

A 3D CAD model and flight hardware of the fully integrated system are shown in Figure 13. The accumulator and pump on the support plate take up only a small portion of the total volume used.

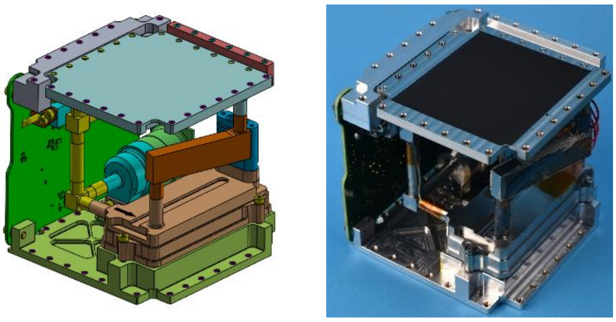

Figure 13. miniMPL Flight Model 3D CAD (left) and final flight hardware (right).

All bolted interfaces are made with structural rigidity in mind. Where possible M2.5 or larger bolts are used with bronze locking helicoils to maximise strength of the connections while avoiding the use of epoxy. Figure 14 shows the orientation of the miniMPL system inside the CubeSat frame. Only the base support plate and the radiator are rigidly connected to the frame to avoid over-constraining the assembly.

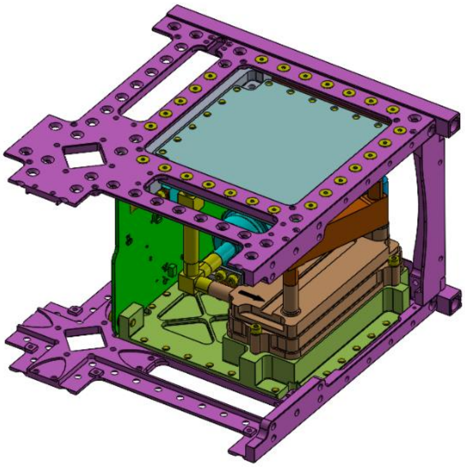

Figure 14. 3D CAD model of miniMPL Flight Model assembly integration into the CubeSat frame.

B. *Filling procedure*

The miniMPL loop is filled with Galden HT55 using a dedicated fill line integrated into the system via a T-joint. This fill line consists of a ⅛” tube extending from the loop and is connected through a set of valves to both a vacuum pump and a fluid reservoir.

The loop is evacuated and subsequently backfilled with Galden HT55 under vacuum to ensure complete filling without trapped gases.

Following initial filling, the required fill level of the accumulator is established. As described in Section III.D, the accumulator operates based on a two-phase equilibrium and must therefore contain both liquid and vapor during operation. To enable this, the effective fill level of the accumulator is set to approximately 50% at ambient conditions.

The desired fill state was established by heating the accumulator to generate vapor and expel excess liquid through the fill line until 50% of the accumulator volume was expelled. Once this fill level was reached, the fill line was mechanically sealed by pinching. To create a permanent hermetic seal, a final weld was applied at the end of the fill tube.

After sealing, the remaining section of the fill line was folded and mechanically secured to prevent movement under launch loads. Tube guides and a hook at the tip of the line were used to constrain the tube, as shown in Figure 15.

Some air remains trapped between the final seal weld and the pinch. However, within the expected operating temperature range the maximum pressure generated by the trapped air is not sufficient to affect structural integrity or operation of the loop.

As the flight loop does not include an internal pressure sensor, direct pressure measurement after filling is not possible. Leak-tightness of the sealing process was verified through representative test articles that were sealed using the same pinch-off and weld procedure and subsequently subjected to helium leak testing. In addition, during thermal vacuum testing, the chamber pressure was continuously monitored for indications of leakage from the loop.

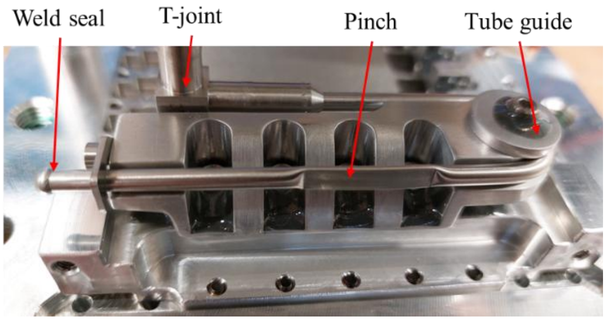

Figure 15. miniMPL Flight Model fill line folded and secured after filling and sealing.

The filling approach used allows the loop to be charged, conditioned, and hermetically sealed using standard fluid handling equipment without requiring dedicated service valves in the final flight configuration. This reduces mass, leakage risk, and overall system complexity.

C. *miniMPL electrical integration*

The miniMPL Flight Model interfaces electrically with the spacecraft platform for both power and data handling. The electrical architecture is designed to be simple and robust, in line with the demonstration nature of the mission.

Power is supplied by the platform power system and distributed to the different subsystems within the miniMPL, including the pump drive electronics, accumulator heater, and dummy heat source. Each subsystem is controlled independently, allowing flexible operation during the in-orbit demonstration.

The drive electronics for the pump are integrated within the system and generate the required high-voltage actuation signals for the piezo elements. No complex command-and-control interface is implemented between the miniMPL hardware and the OBC, however the miniMPL does provide health telemetry through an I^2C interface.

Telecommands received by the spacecraft OBC modify software configuration parameters, which are then interpreted to enable or disable power lines, thereby commanding the hardware accordingly. Figure 16 gives an overview of power and data interfaces with the platform.

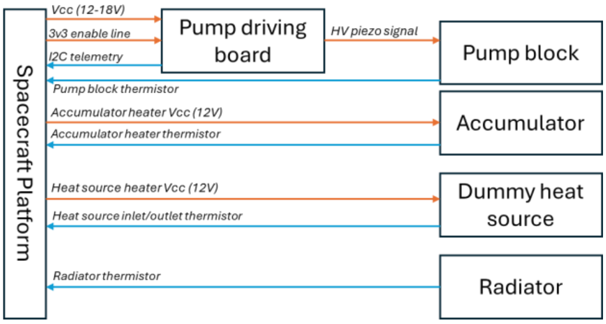

Figure 16. miniMPL Flight Model electrical interface diagram, showing power and data connections to the platform.

No system-level electrical redundancy is implemented beyond the inherent redundancy of the pump and drive electronics architecture. This is considered acceptable for the in-orbit demonstration mission, where the primary objective is technology validation rather than mission-critical operation.

V. QUALIFICATION AND ENVIRONMENTAL TESTING

A. *Vibration Qualification*

The integrated miniMPL Flight Model was subjected to the vibration qualification campaign defined in section II.C. An adapter plate and fixture were designed to mount the miniMPL to the shaker machine. The adapter plate and fixture were designed with sufficiently high stiffness to avoid influencing the response within the tested frequency range. The miniMPL system with its fixture is shown in Figure 17.

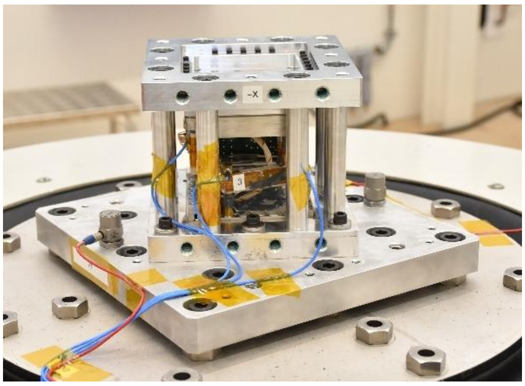

Figure 17. miniMPL Flight Model placed on the shaker plate for vibration testing in the z-axis.

A reference sensor was placed on the adapter plate to determine the actual load applied to the miniMPL. Three sensors were placed on the miniMPL itself to measure acceleration. The locations of these sensors were chosen based on finite element analysis of the miniMPL system.

During the analysis three main modes of vibration were identified within the environmental vibration regime. Figure 18 shows an exaggerated displacement of these three modes. The first mode is an x-direction wobble of the accumulator. To capture this mode, the first accelerometer is placed on the back of the accumulator. The second mode is a y-direction wobble of the joint connecting the accumulator to the rest of the loop, so the second accelerometer is placed there. The final mode is an x-direction wobble of the dummy heat source. The third accelerometer is placed there to capture this displacement. All three modes are within the vibration regime at 1424, 1884, and 1976 Hz. All three of the modes were local modes with effective modal masses below 10% of total system mass.

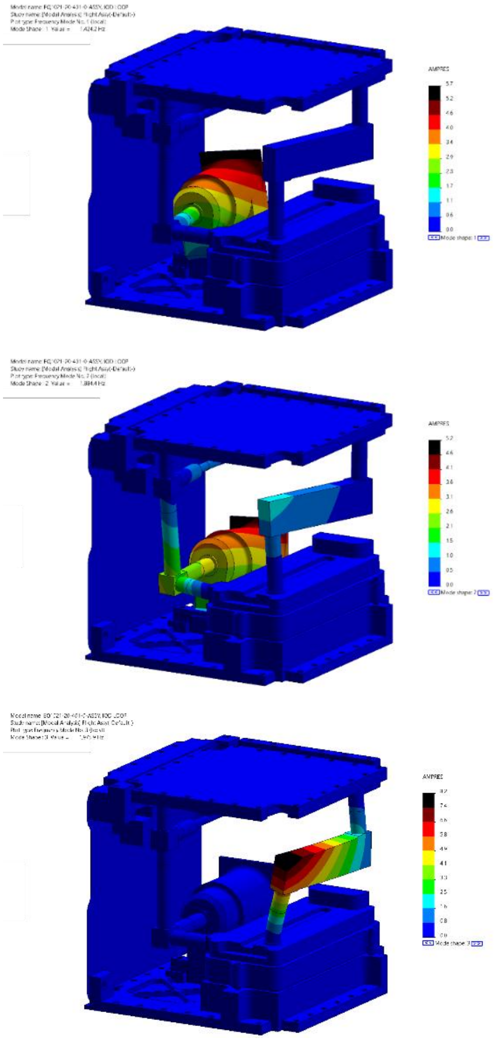

Figure 18. miniMPL Flight Model three local vibration modes at 1424 Hz (x-direction), 1884 Hz (y-direction) and 1976 Hz (x-direction) respectively.

Vibration testing began with a low-level eigenfrequency sweep (2 to 2000 Hz at 0.5 g). The frequency responses from all accelerometers were logged. The qualification vibration profile was then applied, followed by another eigenfrequency sweep. The eigenfrequencies and corresponding amplitudes before and after the vibration regime were compared. Any deviations were recorded and validated against the limits described in ECSS-E-ST-10-03C to determine pass or fail. This was done for all three axes.

Table VI shows the measured modes and change in frequency and amplitude of these modes. It can be seen that both the first and third mode have very small shifts in both frequency and amplitude. Notably, however, a 23% change was observed in the amplitude of the second mode acceleration. At the same time, no significant change in frequency of that mode was observed. This indicates a change in energy transfer to the mode, but no change in stiffness of the structure. The latter finding rules out plastic deformation of structural parts. The most probable cause was settling of the accumulator blade bolted interfaces.

TABLE VI. miniMPL FLIGHT MODEL MEASURED MODE FREQUENCY AND AMPLITUDE CHANGES DUE TO VIBRATION TESTING

Mode #		Frequency [Hz]	Freq. delta	Amplitude [g]	Ampl. delta
1	Pre	1377.8	-1.1%	21.05	-6.4%
	Post	1393.2		19.7	
2	Pre	1872.4	-0.6%	17.07	23%
	Post	1857		21	
3	Pre	1893.2	3.1%	16.8	2.0%
	Post	1951.6		17.14	

Since all modes within the tested range were local modes with effective modal masses below 10%, ECSS-E-ST-10-03C does not impose explicit acceptance criteria for the observed shifts. As the miniMPL functionality was unaffected by the vibration testing and the change in amplitude of the second mode is attributed to settling of a bolt connection, the miniMPL system passed this test.

B. *Thermal vacuum performance testing*

The miniMPL Flight Model integrated system was subjected to thermal vacuum (TVAC) testing in order to verify both its functional performance and structural integrity under representative in-orbit conditions. The applied test conditions are based on the environmental requirements defined in Section II.C, including high vacuum and representative thermal cycling.

The system was mounted inside a thermal vacuum chamber with the support plate having a conductive interface with the chamber cold plate. The system was placed such that heat rejection through the radiator is representative of in-orbit conditions, while minimizing parasitic heat losses through the mounting structure, as shown in Figure 19. Temperature measurements were obtained using the thermistors that are part of the Flight Model. The chamber pressure was reduced to below 1×10^{-5} mbar to ensure vacuum conditions representative of Low Earth Orbit.

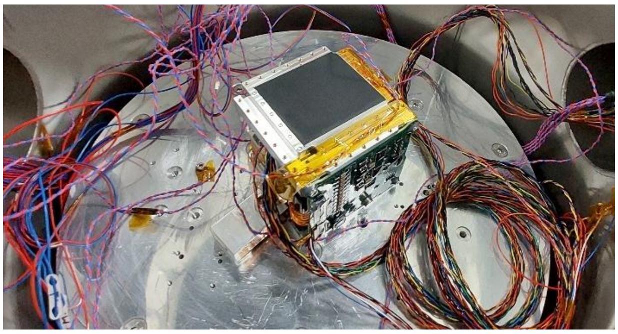

Figure 19. miniMPL Flight Model placed in the TVAC chamber. The support plate has a conductive interface with the cold plate and the radiator has unobstructed view of the TVAC chamber shroud.

Thermal cycling was performed between the defined non-operational and operational temperature limits of the system (see Section II.C). During these cycles, the miniMPL was operated in representative modes, including activation of the pump, accumulator heater, and dummy heat source. This allowed verification of both start-up behaviour and steady-state operation under thermal extremes.

Performance evaluation during TVAC testing focussed on key system parameters, including:

- Temperature distribution across the loop (inlet/outlet of heat source, radiator, pump body, and accumulator),
- Heat transport capability,
- Accumulator thermal stability / inferred pressure
- Electrical power consumption

The primary performance metric was the ability of the system to transport and reject the imposed 5 W heat load under vacuum conditions. The temperature difference between the inlet and outlet of the dummy heat source was used to quantify the effective heat transport, while radiator temperature provided insight into heat rejection efficiency.

In addition to steady-state performance, transient behaviour was evaluated during system start-up and shutdown. Particular attention was given to the interaction between accumulator temperature control and loop temperatures.

It was observed that the accumulator temperature was strongly influenced by conductive heat leakage through the connecting tube rather than solely by the heater input. The temperature of the accumulator, however, was still sufficiently high for stable loop operation.

A second observation was that fluid viscosity had a larger than expected impact on pump performance under low-temperature conditions. Whereas at ambient or higher temperatures the pump performed as expected, at temperatures below 0°C the viscosity of the fluid significantly increased the pressure drop of the loop. This manifested itself as a reduction in mass flow and subsequently an increase in delta-T across the dummy heat source. At -20°C the mass flow was reduced by 50% as shown in Figure 20.

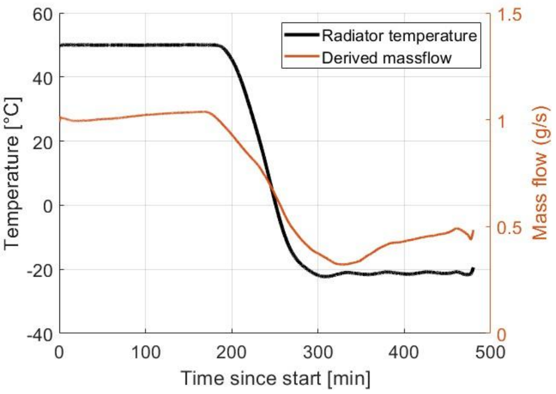

Figure 20. miniMPL Flight Model derived mass flow reading during TVAC testing. Also shown is the radiator temperature.

Aside from these two findings, no permanent degradation in system performance was observed over the course of the thermal cycles. The system successfully demonstrated stable operation, maintaining continuous flow and effective heat transport under all tested conditions. No fluid leakage, structural damage, or measurable degradation was observed during or after completion of the TVAC campaign.

C. *Electromagnetic compatibility testing*

As mentioned in Section II.C.3, EMC verification was limited to emission testing in the radiated and conductive domain. The verification was performed according to the methods defined by ECSS-E-ST-20-07C. The applicable limits are also derived from this ECSS with the addition of the platform-specific receiver bands. The verification tests were performed by the EMC test centre of NLR.

During the conducted emissions tests, the electrical noise through the power and signal lines was measured and compared against the applicable limits. The conductive emission tests included common mode and differential mode emissions on the power and signal lines as well as the inrush current and transient characterisations.

Radiated emissions were recorded over the complete specified spectrum in both polarisations. Dedicated antennas covering parts of the spectrum were used, as shown in Figure 21.

Figure 21. miniMPL Flight Model at the EMC test facility during one of the radiated emission tests at NLR. Note that miniMPL is covered with foil for cleanliness reasons.

Successful completion of the EMC campaign demonstrates that compact high-voltage piezoelectric drive electronics can be implemented within CubeSat-class platforms without unacceptable interference to neighbouring spacecraft subsystems.

D. *miniMPL Flight Model performance summary*

The miniMPL Flight Model system is an integrated heat transport system designed for in-orbit demonstration. Its properties are shown in Table VII.

TABLE VII. miniMPL SYSTEM IN-ORBIT DEMONSTRATION PROPERTIES

Property	**Value**
Pump mass	0.260 kg
Full integrated system mass	0.826 kg
Full integrated system volume	1U
Pump mass flow	Max. 1.2 g/s 0.8 – 1.0 g/s nominal
Pump max pressure head	Max. 300 mbar
Heat source delta-T at nominal flow per W of heat transported	~0.75 °C/W
Input power	1 W (pump) 0.9 W (accumulator)
Min. operating temperature	-30 °C
Max. operating temperature	90 °C
Normal operating pressure	2.8 bara
Design burst pressure	10 bara

VI. FLIGHT READINESS AND IN-ORBIT DEMONSTRATION

Following completion of manufacturing, assembly, and qualification testing, the miniMPL Flight Model has been accepted for payload-level integration into the host spacecraft. Mechanical, electrical, and software interfaces were verified during standalone integration activities, and no open issues remain that would prevent progression to spacecraft-level integration at the time of writing.

The qualification campaign demonstrated compatibility of the integrated system with the expected launch and in-orbit environments. Vibration testing confirmed structural integrity with no loss of functionality. Thermal vacuum testing demonstrated stable loop operation, continuous heat transport, and survivability across the required temperature range. EMC testing confirmed that the piezoelectric drive electronics complied with the applicable emission limits for hosted CubeSat operation.

The planned in-orbit demonstration will provide the first operational assessment of the miniMPL concept in microgravity and representative orbital thermal boundary conditions. Mission objectives include verification of autonomous start-up behaviour, long-duration flow stability, accumulator pressure regulation through temperature control, and repeatable rejection of a controlled internal heat load through the radiator.

Telemetry acquired during flight will be used to compare measured performance with pre-flight thermal and hydraulic models. The mission therefore serves both as a technology demonstration and as a validation step for future miniMPL designs intended for operational spacecraft applications.

VII. CONCLUSIONS AND FUTURE WORK

This paper presented the first Flight Model of the mini Mechanically Pumped Loop (miniMPL), a compact active thermal control system developed for CubeSat- and small-satellite-class spacecraft. The demonstrated hardware integrates a redundant piezoelectric pump, two-phase accumulator, compact radiator, representative heat source, and drive electronics, within a 1U payload allocation with a total mass below 1 kg.

Ground qualification and functional testing confirmed that the integrated system can operate within the mechanical, thermal, vacuum, and electromagnetic constraints associated with small satellite missions. Stable loop circulation was demonstrated with pump flow rates up to 1 g/s under orbital thermal conditions, providing controlled transport of the representative mission heat load.

These results indicate that mechanically pumped thermal control can be realized within the mass, volume, and power limitations of modern CubeSat platforms. This enables future missions with increasing onboard power densities, localized hot spots, distributed payloads, or thermal requirements that exceed the practical limits of passive control approaches.

Future work will focus on in-orbit performance assessment, reduction of parasitic thermal coupling, improved low-temperature hydraulic performance, higher electrical efficiency, and scaling of the architecture toward greater heat transport capacity and multiple heat load configurations.

The miniMPL Flight Model therefore represents an important step toward practical and standardized active thermal control solutions for next-generation small spacecraft.

VIII. REFERENCES

[1] B. Lal, Global trends in small satellites, Alexandria: IDA Science and Technology Policy Institute, 2017.

[2] T. V. Ganzeboom, J. van Es, T. van den Berg, A. van Vliet, H. Brouwer, S. Elvik, G. Giammaria, R. Kunst and M. Arendshorst, “Mini Mechanically Pumped Loop for standardized small satellite thermal control: Engineering Model design manufacturing and testing,” in *54th International Conference on Environmental Systems*, Prague, 2025.

[3] H. Gerner, R. van Benthem and J. van Es, “Fluid Selection For Space Thermal Control Systems,” in *International Conference on Environmental Systems*, Tucson, Arizona, 2014.

[4] T. Ganzeboom, J. van Es and L. Formisani, “Development of a miniature heat exchanger for mechanically pumped loop systems for active thermal control of CubeSats,” in *51st International Conference on Environmental Systems*, St. Paul Minnesota, 2022.

[5] S. de Jong, T. Ganzeboom, S. Elvik and H. Brouwer, “Mechanically Pumped Loop As Heatsink Solution For Advanced Onboard Data Processors,” in *European Data Handling & Data Processing Conference For Space*, Juan-Les-Pins - France, 2023.